TRANSMISSION LINE MODELS FOR THE SIMULATION OF INTERACTION PHENOMENA BETWEEN PARALLEL AC AND DC OVERHEAD LINES

Bjørn Gustavsen
SINTEF Energy Research
Trondheim, Norway

Garth Irwin
Manitoba HVDC Research Centre
Winnipeg, Canada

Ragnar Mangelrød
Norwegian Power Grid Company (Statnett SF)
Oslo, Norway

Dennis Brandt
Siemens AG
Erlangen, Germany

Kelvin Kent
Manitoba Hydro
Winnipeg, Canada

Abstract – The paper discusses the merit of different transmission line models in terms of accuracy and efficiency, followed by a description of the implementation of a phase domain line model in an EMTP-type program. Topics included are: model formulation, least squares curve fitting, time delay identification and convolutions. The implemented model is demonstrated to give highly accurate results for the simulation of low frequency coupling effects between parallel overhead lines.

1 INTRODUCTION

Parallel AC and DC overhead lines are present in several HVDC projects currently under development, for instance in southern Norway, and in the 3-Gorges project in China. It is known that coupling between the AC and DC line can lead to undesirable interaction phenomena, which may affect system control and protection, and possibly the lifetime of the converter transformers [1].

Traditionally, the most accurate transmission line models have been based on a constant transformation matrix with frequency dependent modes. This type of model may give satisfactory results for situations involving high frequency transients, but the accuracy often deteriorates in the low frequency area due to frequency dependency of the transformation matrix (unbalanced lines).

An investigation revealed that line models based on a constant transformation matrix will in many situations not simulate interaction with sufficient accuracy. It was therefore decided to implement a new standard transmission line model in EMTDC which is fully general and accurate, at all frequencies. A recently proposed phase domain model [2] was selected as basis for this purpose. This paper describes practical aspects related to its implementation, and demonstrates its suitability for simulation of interaction phenomena.

2 REVIEW OF TRANSMISSION LINE MODELS

Accurate transmission line modeling requires that the frequency dependent effects of the line are taken into account. At present, there are three main categories of line models which have the potential of achieving this :

- Exact pi-model
- Traveling wave model with modes
- Traveling wave model in phase domain

For these models it is necessary to approximate a set of frequency responses with rational functions, in order to achieve high computational efficiency for the time domain convolutions. The set of frequency responses is different for the different line models.

Exact pi-model [3]
The elements of the pi-model are oscillating functions in the frequency domain due to the time delays of the line. Although it is possible to fit these functions with rational functions, the order can become very high when considering a long line (or wide frequency range). The high order would make this model time consuming in the time domain simulations.

Traveling wave models
The traveling wave method is the preferred approach because the time delays can with this approach be extracted from the functions to be fitted (backwinding), thus allowing a low order model. In addition, decoupling between the two line ends allows further savings in the time domain when it is necessary to update the system admittance matrix (due to non-linear circuit elements).

Traveling wave model in the modal domain
The existing frequency dependent line models in EMTDC are based on the traveling wave approach with frequency dependent modes and a constant transformation matrix, with an implementation similar to [4]. However, as is shown in section 4, this model is sometimes unable to simulate low frequency coupling effects with sufficient accuracy.

In principle, this deficiency can be overcome by including the frequency variation of the transformation matrix in the simulation [5]. Although this approach gives accurate results for cable systems, it is in general not applicable to overhead lines because the modal decomposition is sometimes unstable [6].

Traveling wave model in the phase domain
The problem of a frequency dependent transformation matrix can be overcome by formulating the model directly in the phase domain (without diagonalization). With this method it is necessary to fit in the phase domain the matrix elements of the propagation function $H(\omega)$ and the characteristic admittance $Y_c(\omega)$. The elements of $Y_c(\omega)$ are smooth functions of frequency and can easily be fitted.

The fitting of $H(\omega)$ is more difficult because its elements contains modal contributions with different time delays. In several contributions [7-8] it has been suggested to extract from each element of $H(\omega)$ a single time delay. However, the uncompensated part of the time delays may result in an oscillating behavior in the frequency domain. For

lines with high ground resistivity a large number of oscillations may occur, thus requiring a high order fitting.

The problem of different time delays in $H(\omega)$ can be overcome by including modal time delays in the phase domain. Four line models have been proposed which achieve this :

- ARMA Model (z-domain)
- Idempotent Line Model (s-domain)
- Polar Decomposition Model (s-domain)
- Universal Line Model (s-domain)

The ARMA Model [9], which has already been implemented in ATP-EMTP, is based on fitting the elements of H (and Y_c) in the z-domain, with time delays obtained from the modes. Although the method appears attractive, its usage of z-domain fitting makes it necessary to refit the elements of H (and Y_c) whenever the user wants to change the time step of the simulations. This is inconvenient from a practical point of view, and so an s-domain approach is preferred.

The Idempotent Line Model [10] expands H into a sum, where each term is given as an idempotent matrix M multiplied with a corresponding mode. The rational approximation of H is obtained by fitting the modes *and* the idempotents. However, we have found that in some cases of overhead line modeling, unstable poles are needed in order to achieve accurate fitting for M.

The Polar Decomposition Model [11] has a kernel (diagonal matrix) containing poles and time delays from the modes, which is multiplied by two rectangular matrices C and B. The difficulty with this model is the identification of C and B due to the non-linear nature of the problem. Although "BC-iterations" gave quite accurate results, the optimal solution was probably not obtained.

The Universal Line Model [2] is based on calculating unknown residues when the poles and time delays have been precalculated from the modes. All poles are assumed to contribute to all elements of H, but without the usage of idempotents or a pole sharing kernel. This model has been found to give highly accurate results and was therefore selected as basis for a new standard model for EMTDC.

3 IMPLEMENTATION OF PHASE DOMAIN MODEL

The Universal Line Model has been described in [2]. The following reviews the main elements of the model and highlights some practical aspects related to its implementation.

3.1 Frequency domain fitting

Approximation with rational functions

As part of the transmission line project, a least squares fitting routine, Vector Fitting (VF) [12], was implemented as a FORTRAN subroutine. The resulting fitting will in general contain both real and complex poles, depending on the shape of the frequency response. All poles are stable.

Backwinding, collapsing, and fitting the modes of $H(\omega)$

The modes of $H(\omega) = \exp(-\sqrt{YZ}\,l)$ are calculated via a frequency dependent transformation matrix, T. T is obtained by the Newton-Raphson approach described in [13]. (Usage of a constant real T was found to give less accurate results for the phase domain fitting of H).

Each mode is "backwinded" by multiplication with $\exp(s\tau_i)$, and the resulting function is finally fitted using VF :

$$e^{s\tau_i} H_i^m(s) = \sum_{m=1}^{N} \frac{c_m}{s - a_m} \qquad (1)$$

Unlike asymptotic magnitude fitting [4], VF requires both the magnitude and phase angle of the mode to be known before the fitting can be done. Thus, the time constant for backwinding must be precalculated. A suitable time constant is calculated based on the technique in [6]. This method is based on a furmula by Bode, which for a minimum-phase-shift function relates the magnitude function to the phase angle.

Significant improvements have been made to the backwinding procedure in [6] :

- Previously, "Ω" in figure 2 of [6] was selected as the frequency where the magnitude function has decayed to 0.1. In the present implementation, Ω is chosen as the frequency where the magnitude function has decayed to "*errmode*", with *errmode* as defined in section 3.4.
- The time delays are finally subjected to an *iterative refinement* in which the modes are refitted several times, each time with an improved time delay. A simple search method is used in the iterations.

Modes with nearly equal time delays are replaced with a single mode equal to the average of the modes. An associated time delay is calculated in the same way as for the uncollapsed modes.

Fitting $H(\omega)$ in the phase domain

With the poles and time delays of the modes known, $H(\omega)$ is finally fitted in the phase domain (calculation of residues). Each element is on the form :

$$h(s) = \sum_{i=1}^{Ng} \left(\sum_{m=1}^{N} \frac{c_{m,i}}{s - a_{m,i}} \right) e^{-s\tau_i} \qquad (2)$$

Because the modes are fitted independently, poles of different modes may accidentally come very close. If this happens at low frequencies (were the time delays are of little significance), the respective residues for the phase domain fitting can become very large (with opposite sign). This can potentially cause instabilities in the time domain solution due to roundoff errors. Therefore, a warning is issued if the ratio between residue and pole (c/a) is larger than a threshold value, which at present is set to 100. If this happens, then one should consider to refit the modes with a different order. The probability of large residues occurring increases with increasing order of the fitting.

Fitting $Y_c(\omega)$ in the phase domain

Initially, the special vector fitting capability of VF was used to fit $Y_c(\omega)$ columnwise using an identical set of poles. However, as VF has been implemented without usage of a sparse solver, the memory requirement was found to be excessive for situations with a large number of conductors.

This problem was solved by using the same lumping technique as for $H(\omega)$. Because $Y_c(\omega)$ has no time delays, a suitable set of poles can be obtained by fitting the sum of *all* modes. Furthermore, for a (square) matrix A with eigenvalues λ we have the relation [14] :

$$\sum_{i=1}^{N} \lambda_i = \sum_{i=1}^{N} A_{ii} \tag{3}$$

Thus, instead of fitting the sum of modes we can instead fit the sum of the diagonal elements of $Y_c(\omega)$.

The sum is fitted using VF with an approximation of the form

$$f(s) = d + \sum_{m=1}^{N} \frac{c_m}{s - a_m} \tag{4}$$

Finally, the elements of $Y_c(\omega)$ are fitted in the phase domain using the poles from (1) as known quantities. Similarly as for $H(\omega)$, all elements of $Y_c(\omega)$ get identical poles.

Solution technique for least squares problem

A linear least squares solver is needed both in VF and when calculating the residues of $H(\omega)$, and the residues and constant term of $Y_c(\omega)$. For this purpose we use QR decomposition with rank revealing column pivoting. This method gives excellent results also in situations when the problem is not of full numerical rank. Usage of singular value decomposition (SVD) is more time consuming.

3.2 Time domain implementation

The traveling wave equations are interfaced to the main program by means of the usual Norton Equivalent in fig. 1.

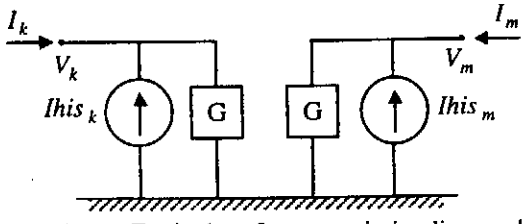

Fig. 1 Norton Equivalent for transmission line model

Figure 2 shows an overview of how the updating of $Ihis_k$ is carried out. V_k and V_m are calculated by the EMTDC main program and read into the transmission line subroutine. Subscripts i and r denote incident and reflected waves, respectively.

$$\begin{aligned} I_k(n) &= GV_k(n) - Ihis_k(n) \\ I_{kr}(n) &= I_k(n) - I_{ki}(n) \\ I_{ki}(n+1) &= H * I_{mr}(n-\tau) \\ Ihis_k(n+1) &= Y_c' * V_k(n) - 2I_{ki}(n+1) \end{aligned}$$

Fig. 2 Updating $Ihis_k$ in figure 1

Two alternative methods have been implemented for evaluation of the convolution integrals in figure 2 (denoted by '$*$') :

1) trapezoidal integration
2) recursive convolutions [15] assuming linear variation between the voltage samples of the driving functions (V, i_r).

Method 1) and 2) give identical expressions in the time domain, but with different numerical values for the coefficients.

Convolution integral for characteristic admittance

For simplicity we now consider the case of a first order fitting (one pole). The convolution of (4) with an input u $(y = f * u)$ becomes :

$$\begin{aligned} x(n) &= \alpha\, x(n-1) + \lambda\, u(n) + \mu\, u(n-1) \\ y(n) &= c\, x(n) + d\, u(n) \end{aligned} \tag{5}$$

The definition of the coefficients α, λ and μ are given in Appendix A (trapezoidal integration), and in equation (A.6) of [15] (recursive convolution).

However, (5) cannot be implemented in this form because the state variable x depends on the input at the same time instant. This problem is solved by introducing a modified state variable :

$$x'(n) = x(n) - \lambda\, u(n) \tag{6}$$

which gives the following result :

$$\begin{aligned} x'(n) &= \alpha\, x'(n-1) + (\alpha\lambda + \mu) u(n-1) \\ y(n) &= c\, x'(n) + (d + c\lambda) u(n) \end{aligned} \tag{7}$$

Equation (7) can be simplified by scaling the input :

$$\begin{aligned} x''(n) &= \alpha x''(n-1) + u(n-1) \\ y(n) &= c' x''(n) + G u(n) \end{aligned} \tag{8}$$

where

$$c' = c(\alpha\lambda + \mu) \tag{9}$$

$$G = d + c\lambda \tag{10}$$

When there are more than one pole, x'' becomes a vector (array). Note that elements of the state vector can be complex due to complex poles. However, because complex poles always come in conjugate pairs, the output of $c''x'(n)$ is real. Thus, the history current sources are real quantities.

Convolution integral for propagation function

In general, the time delay τ of a given delay group will not be an integer multiple of the time step length Δt used in the simulation. This makes it necessary to interpolate between the sample points of the reflected current waves.

The travel time can be written

$$\tau = (k + \varepsilon)\Delta t \tag{11}$$

where k is an integer and ε is a real number between 0 and 1. The updating of the state variable in (5) for propagation now becomes :

$$x(n) = \alpha\, x(n-1) + \lambda\, u(n-(k+\varepsilon)) + \mu\, u(n-(k+1+\varepsilon)) \quad (12)$$

A modification of the state variable and scaling of the input gives the final result :

$$x''(n) = \alpha\, x''(n-1) + u(n-(k+1+\varepsilon))$$
$$y(n) = c'\, x''(n) + G\, u(n-(k+\varepsilon)) \quad (13)$$

where

$$c' = c(\alpha\lambda + \mu) \quad (14)$$

$$G = c\lambda \quad (15)$$

The interpolated values in (13) are calculated by linear interpolation, as indicated by blank dots in figure 3. Calculation of an interpolation point is done at the cost of one multiplication and 2 additions. The function is assumed to vary between the points as indicated by the dotted line.

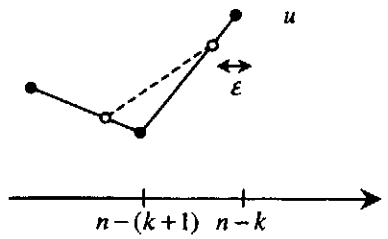

Fig. 3 Linear interpolation

An alternative approach (figure 4) was also considered where the point at $n-(k+1)$ is included in the interpolation. However, the increased accuracy was small and does probably not justify the fact that an additional term must be included in the updating of the state variable (x) in (10).

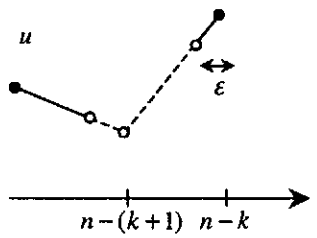

Fig. 4 Alternative interpolation scheme

3.3 Time step loop considerations

Columnwise realization

Because all elements in each column of $H(\omega)$ and $Y_c(\omega)$ have identical poles, a special columnwise realization for the convolutions is possible. The quasi-code below shows the updating of the history current source for end "k" of the line, due to the characteristic admittance.

Note how the property of identical poles has made it possible to "pull out" the updating of the state variables (x) from the row-loop. This reduces the number of floating point operations in the inner-loop from 4 to 2. A similar result is obtained for the propagation function.

```
for col=1:Nc
  for m=1:N
    x(m,col)=α(m,col)*x(m,col)+Vk(col)
  end
end

for col=1:Nc
  Ihisk(col)=0
  for row=1:Nc
    for m=1:N
      Ihisk(col)=Ihisk(col)
                 -c(m,row,col)*x(m,col)
    end
  end
end
```

Elimination of high frequency poles

Poles satisfying

$$\text{abs}(a) > \frac{10\pi}{\Delta t} \quad (16)$$

are not included in the time domain simulation, as their time constants will in any case not be resolved by the given time step. This feature increases the effieciency of the time domain simulation..

When neglecting a pole, it is necessary to modify G (in (10) or (15)) as follows :

$$G' = G + c/a \quad (17)$$

3.4 User Interface

For the fitting of $Y_c(\omega)$ and $H(\omega)$ the user has to specify :
N_{min} : Minimum number of poles
N_{stop} : Maximum number of poles
errlim : error tolerance

Fitting $Y_c(\omega)$:

The fitter starts with a number $N = N_{min}$ poles and increments N until the error is below *errlim*, or N_{stop} is reached. A relative error measure is used for $Y_c(\omega)$.

Fitting $H(\omega)$:

The fitting of $H(\omega)$ is more delicate because there is no unique relation between the accuracy of the modes and the accuracy of $H(\omega)$. The approch adopted is as follows : The modes (groups) are each fitted to an accuracy *errmode*, and $H(\omega)$ is fitted using the resulting poles and time delays. If the required accuracy for $H(\omega)$ is not met, *errmode* is reduced and the process is repeated until the required accuracy (*errlim*) is achieved (or until $N = N_{stop}$).

Weighting :

The accuracy of the least squares fitting can be modified by using different weighting at different frequency intervals. For instance, a very high weight may be used at power frequency to ensure correct load flow.

4 CALCULATED RESULTS

4.1 Line geometry

As an example we consider a 500 kV DC line in parallel with a 300 kV AC line. The line length is 25 km, and the ground resistivity is is 1000 Ωm. The lines are untransposed.

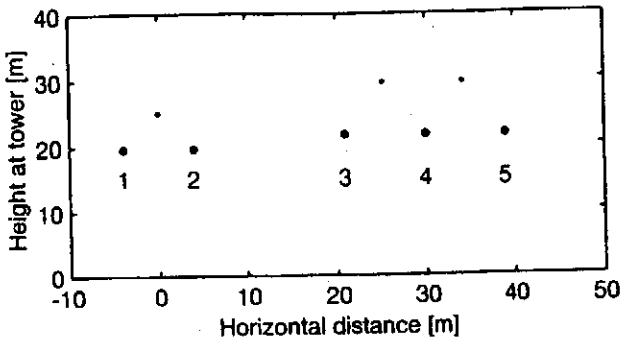

Fig. 5 Parallel DC and AC line

4.2 Balanced line simulation

Frequency dependent line models with a constant transformation matrix can give correct results when the line is assumed to be perfectly transposed, as the transformation matrix is then real and constant.

In the following we neglect the DC line, and assume the AC line to be perfectly transposed. One of the conductors is energized with a 50 Hz voltage source at peak value, as shown in figure 6.

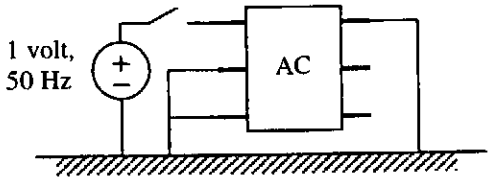

Fig. 6 Energization of transposed AC line

Figure 7 shows the simulated voltage on one of the non-energized conductors, at the receiving end. The voltage is shown when calculated by the modal domain model (dashed line), and by the phase domain model (solid line). As expected, the deviation between the two voltages is small.

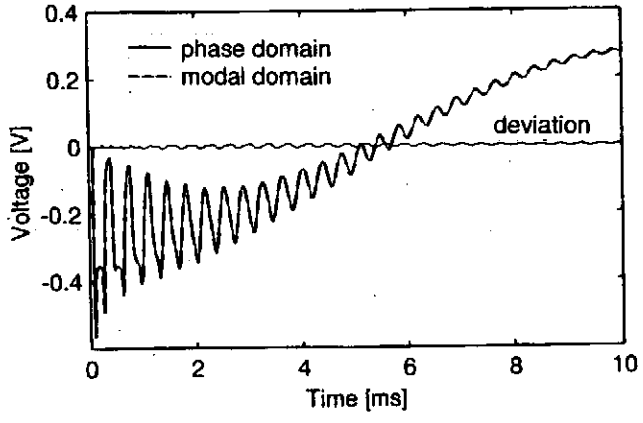

Fig. 7 Simulated voltage on non-energized conductor, at receiving end

4.3 Unbalanced line simulation

For unbalanced (untransposed) lines, simulations by modal domain models may produce incorrect results due to the frequency variation of the transformation matrix. The errors may in some instances become unacceptably large, for instance when calculating inducing effects between parallel overhead lines.

We consider the configuration in figure 5, when none of the lines are transposed. In both the phase domain and modal domain models, the frequency dependent quantities were fitted in the range 0.1 Hz to 1 MHz.

Figures 8 and 9 show the fitted elements of H and Y_c, for the phase domain model. A weighting of 10 was used for the samples between 0.1Hz and 50 Hz, in order to produce a very high accuracy at low frequencies. Y_c was fitted with 17 poles (per column), while H was fitted with 30 poles (per column). The approximations are seen to be very accurate.

For the modal domain model, the tranformation matrix was calculated at 50 Hz, and the modes were fitted using a high order approximation. Also in this case was a weighting of 10 used for the least squares fitting between 0.1 Hz and 50 Hz.

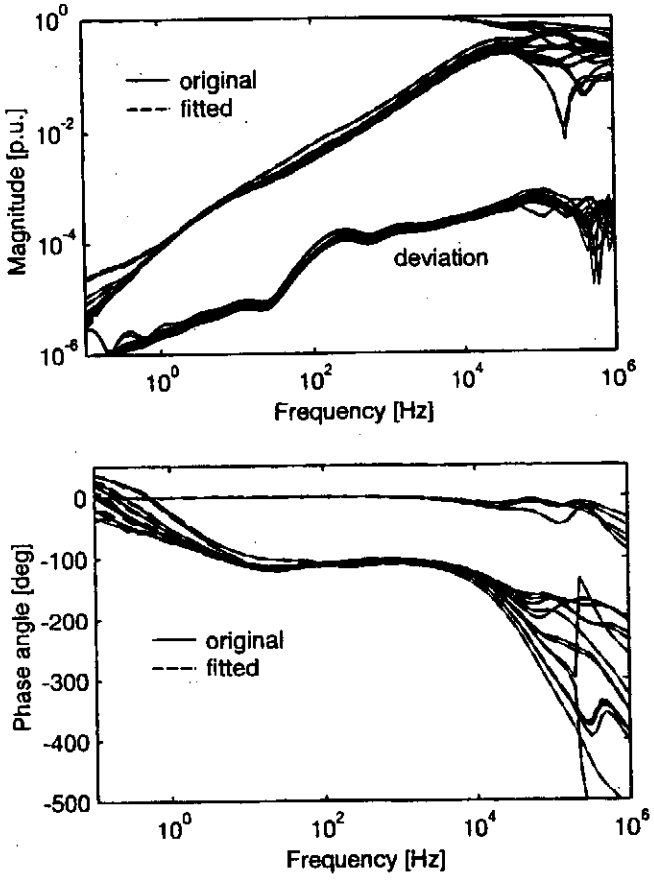

Fig. 8 Fitted elements of $H(\omega)$

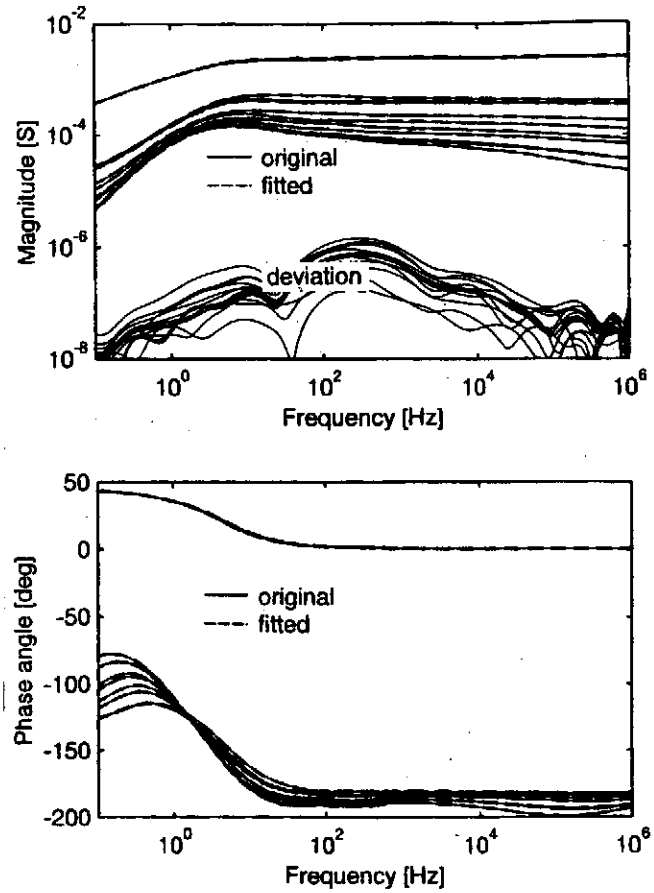

Fig. 9 Fitted elements of $Y_c(\omega)$

Induction of harmonics from DC line to AC line

With the DC line in monopolar operation, the induction effect from a 1A 12th order harmonic current in the DC line on the AC line was investigated using the circuit in figure 10.

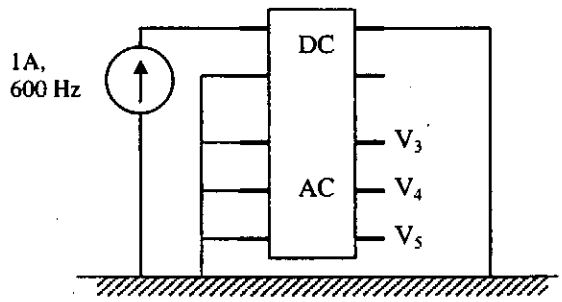

Fig. 10 Induction from 12th order harmonic current

Table 1 shows the magnitude of the voltage on the receiving end of the AC line. The voltages have been calculated by both the modal domain and the phase domain model. The simulated voltages are compared to a theoretically accurate solution calculated in the frequency domain. The voltages by the phase domain are accurate to better than 1%, whereas the modal domain model gives errors as high as 35%.

Table 1 Calculated voltages on AC line

	$\|V_3\|$ [volt]	$\|V_4\|$ [volt]	$\|V_5\|$ [volt]
Theoretical	27.49	21.85	20.34
Phase domain	27.38	21.77	20.29
Modal domain	17.92	27.74	19.01

Table 2 shows the same result, but with the DC line in bipolar operation (no ground return). The induced voltages are now much smaller. As a result the relative errors by the modal domain model become very large, but they are still small for the phase domain model.

Table 2 Calculated voltages on AC line – Bipolar operation.

	$\|V_3\|$ [volt]	$\|V_4\|$ [volt]	$\|V_5\|$ [volt]
Theoretical	5.51	2.96	1.88
Phase domain	5.55	2.96	1.86
Modal domain	10.20	6.10	15.26

Induction from DC current

Theoretically, a DC current in the DC line will not induce any voltage along the AC line. However, inaccuracies in the fitting may result in an artificial coupling between the two lines. This coupling can be unacceptable as the resulting DC currents may saturate transformers in the AC system.

We now calculate the induced DC currents flowing in the AC line, due to a DC current in the DC line. The circuit is shown in figure 11.

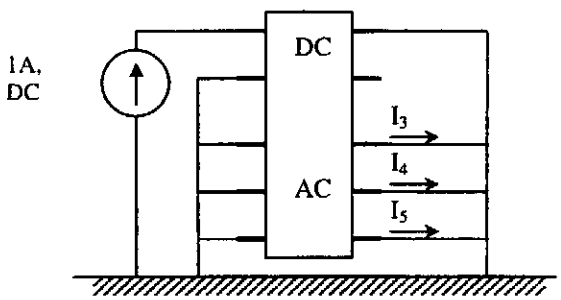

Fig. 11 Induction from DC current

Figure 12 shows the simulated currents in the AC line, when the DC current is ramped up to 1 A in 1 second. It is seen that the stationary currents by the phase domain model are much smaller than those by the modal domain model.

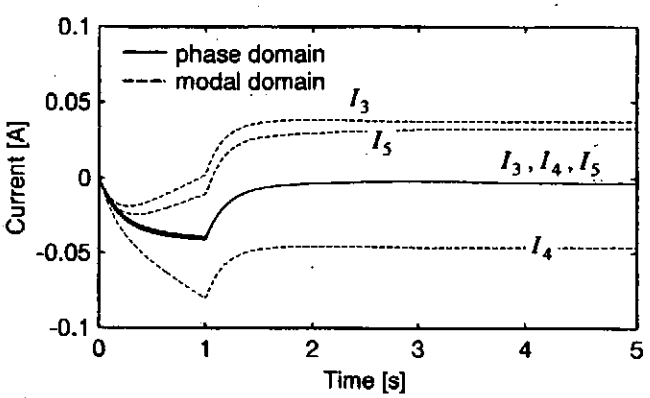

Fig. 12 Induced currents in AC line

Zero sequence induction from AC line to DC line

The inductive effect from a 50 Hz zero squence current in the AC line was calculated using the circuit in figure 10.

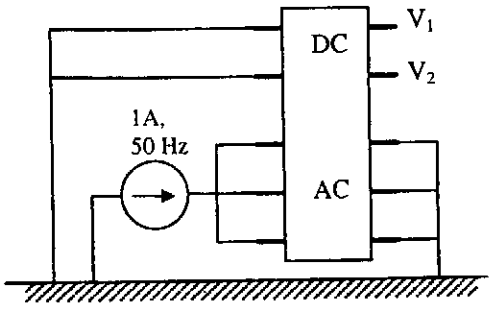

Fig. 10 Induction from 50 Hz current with ground return

Table 3 shows the magnitude of the voltage on the receiving end of the DC line, as calculated by the modal domain and the phase domain model. In this case both models give good results. The increased accuracy for the modal domain model is due to the fact that the transformation matrix was calculated for the same frequency as that of the inducing current (50 Hz).

Table 1 Calculated voltages on DC line

	$\|V_1\|$ [volt]	$\|V_2\|$ [volt]
Theoretical	3.09	3.31
Phase domain	3.06	3.28
Modal domain	2.85	3.37

5 CONCLUSIONS

The paper has described the successful implementation of a phase domain transmission line model in an EMTP-type program. Important features of its implementation include:

Fitting $H(\omega)$

- Calculation of modes for H by a frequency dependent transformation matrix
- Calculation of time delays by an iterative procedure
- Collapsing of modes with nearly equal time delays
- Calculation of poles using a least squares technique (VF).
- Final fitting of H in the phase domain, with poles and time delays as known quantities.

Fitting $Y_c(\omega)$

- Obtaining poles by fitting the sum of diagonal elements of Y_c, using VF
- Final fitting of Yc in the phase domain, with poles as known quantities.

Time domain implementation

- Columnwise realization for convolution of H and Y_c
- Choice between recursive convolution and trapezoidal integration

Simulated results show that

- The phase domain model simulates the coupling between the AC line and DC line with a high degree of accuracy.
- The modal domain model may lead to inaccurate coupling of harmonics from the DC line to the AC line. Also, a DC current may be induced into the AC-line.

6 REFERENCES

[1] E.V. Larsen, R.A. Walling and C.J. Bridenbaugh, "Parallel AC/DC transmission lines steady state induction issues", IEEE Trans. PWRD, vol. 4, no. 1, January 1989, pp. 667-674.

[2] A. Morched, B. Gustavsen and M. Tartibi, "A universal line model for accurate calculation of electromagnetic transients on overhead lines and cables", paper PE-112-PWRD-0-11-1997.

[3] A. Budner, "Introduction of frequency-dependent line parameters into an electromagnetic transients program", IEEE Trans. PAS, vol. 89, no. 1, January 1970, pp. 88-97.

[4] J.R. Marti, "Accurate modelling of frequency-dependent transmission lines in electromagnetic transient simulations", IEEE Trans. PAS, vol. 101, no. 1, January 1982, pp. 147-157.

[5] L. Marti, "Simulation of transients in underground cables with frequency-dependent modal transformation matrices", IEEE Trans. PWRD, vol. 3, no. 3, July 1988, pp. 1099-1110.

[6] B. Gustavsen and A. Semlyen, "Simulation of transmission line transients using Vector Fitting and modal decomposition", IEEE Trans. PWRD, vol. 13, no. 2, April 1998, pp. 605-614.

[7] H.V. Nguyen, H.W. Dommel, and J.R. Marti, "Direct phase-domain modeling of frequency-dependent overhead transmission lines", IEEE Trans. PWRD, vol. 12, no. 3, July 1997, pp. 1335-1342.

[8] B. Gustavsen and A. Semlyen, "Combined phase and modal domain calculation of transmission line transients based on Vector Fitting", IEEE Trans. PWRD, vol. 13, no. 2, April 1998, pp. 596-604..

[9] T. Noda, N. Nagaoka and A. Ametani, "Phase domain modeling of frequency-dependent transmission lines by means of an ARMA model", IEEE Trans. PWRD, vol. 11, no. 1, January 1996, pp. 401-411.

[10] F. Castellanos, J.R. Marti and F. Marcano, "Phase-domain multiphase transmission line models", International Journal of Electrical Power & Energy Systems, vol. 19, no. 4, May 1997, pp. 241-248.

[11] B. Gustavsen and A. Semlyen, "Calculation of transmission line transients using Polar Decomposition", IEEE Trans. PWRD, vol. 13, no. 3, July 1988, pp. 855-862..

[12] B. Gustavsen and A. Semlyen, "Rational approximation of frequency domain responses by Vector Fitting", IEEE paper PE-194-PWRD-0-11-1997, presented at the IEEE/PES Winter Meeting, Tampa, 1998.

[13] L.M. Wedepohl, H.V. Nguyen and G.D. Irwin, "Frequency-dependent transformation matrices using Newton-Raphson method", IEEE Trans. PWRS, vol. 11, no. 3, pp. 1538-1546.

[14] L.N. Trefethen and D. Bau, "Numerical linear algebra", SIAM, Philadelphia, 1997, pp. 186.

[15] A. Semlyen and A. Dabuleanu, "Fast and accurate switching transient calculations on transmission lines with ground return using Recursive Convolutions", IEEE Trans. PAS, vol. 94, March/April 1975, pp. 561-571.

7 APPENDIX

A — Trapezoidal integration

For (3) we get with trapezoidal integration :

$$\alpha = (1 + a\Delta t/2)/(1 - a\Delta t/2) \qquad (A.1)$$

$$\lambda = \mu = (\Delta t/2)/(1 - a\Delta t/2) \qquad (A.2)$$